BULLETIN OF THE POLISH ACADEMY OF SCIENCES
TECHNICAL SCIENCES, Vol. 73(2), 2025, Article number: e152708
DOI: 10.24425/bpasts.2024.152708

Research on fire smoke traceability based on emotional intelligence Jaya algorithm

Xiaoxiao LIU [1], Wenhan ZHONG [2], Tao DING [1] *, Luyao LIN [1], Jinxia MU [1], Jianghuan SHI [3], and Zesong LI [3]

[1] China Jiliang University, China
[2] Zhejiang Light Industrial Products Inspection and Research Institute, China
[3] Ningbo Institute of Measurement and Testing, China

Abstract. To timely detect fire smoke in the early stages and trace the gas generated, thereby avoiding the loss of human life and property and reducing damage to the ecological environment, this paper proposes a fire smoke tracing method based on the emotional intelligence Jaya algorithm (EIJaya). The algorithm assigns an anthropomorphic mental state to the unmanned aerial vehicle (UAV) in the traceability task to realize its self-evaluation and social evaluation. In the simulation concentration field, the EIJaya algorithm, the basic Jaya algorithm, and the PSO algorithm were used for the verification of the simulation of gas traceability, and the simulation results proved the advantages of the EIJaya algorithm in terms of the success rate and the iteration times. In this paper, the TT UAV was chosen as an experimental tool to utilize the functions of its expansion module fully, and the experimental hardware system was constructed by combining it with the corresponding sensors. The corresponding experimental scene was built in the indoor environment, and the EIJaya algorithm was used to make multiple UAVs cooperate and conduct traceability experiments, which verified the algorithm feasibility in practical applications and proved that the algorithm could quickly and accurately trace the fire smoke.

Keywords: fire smoke; gas traceability; EIJaya algorithm; UAV.

1. INTRODUCTION

When a fire occurs, the smoke produced by combustion releases a series of iconic gases, including carbon monoxide (CO), carbon dioxide (CO_2), and nitrogen oxides (N_xO_y). Gas traceability technology can trace these signature gases, and the location of the fire point can be effectively deduced to achieve the accurate positioning of the fire scene.

Gas traceability methods are divided into traditional traceability and active traceability. Traditional traceability methods include sensor networks [1] and biological detection methods [2]. Sensor networks require a certain amount of cost and resource investment to install, calibrate, and maintain sensor nodes. Complex environments and large-scale monitoring may affect positioning accuracy and sensor networks also face specific challenges for long-term and large-scale monitoring, such as battery life, data storage, and transmission. Biological detection is a traceability method that uses organisms, such as insects and search and rescue dogs, to sniff the odour in the smoke and indicate the location of the fire point. Biological detection methods are limited by the quality of training and individual differences in organisms that can affect the method reliability and environmental factors in practical applications. For example, insect activity is limited by weather conditions and seasonal changes, and sniffer dogs have difficulty searching for large-scale and complex environments. In addition, training living organisms takes time and effort and requires professional guidance and handling.

Given the limitations of traditional traceability methods, active olfaction technology has become an important development direction in gas traceability in recent years. In 1984, Larcombe *et al.* [3] proposed reducing the risk of personnel exposure to hazardous environments by using robots carrying various sensors to work in radiation fields and operating them remotely. In 1991, Rozas *et al.* [4] proposed developing a chemical gradient tracking algorithm for source localization of gas plumes. By analyzing the concentration and distribution pattern of the gas, the robot can determine the source and direction of specific gases. In 1992, Genovese *et al.* [5] achieved mutual communication and coordinated action between robots by using mobile micro-robot groups, sensors, and communication technologies, forming a self-organizing behaviour pattern for searching and tracking pollution sources. This method can effectively detect large-scale pollution sources in complex environments and proves the advantages of self-organizing behaviour and robot groups in traceability, which is better than applying a single robot. This early research work laid a good foundation for developing active olfaction technology.

With the continuous advancement of UAV technology, its compactness and flexibility show significant advantages in active olfaction [6]. Since the 1990s, researchers have gradually recognized and enhanced gas traceability technology based on UAVs at home and abroad [7–9]. However, in complex situations, more than a single UAV traceability system is needed

*e-mail: dingtao@cjlu.edu.cn

Manuscript submitted 2024-07-28, revised 2024-10-06, initially accepted for publication 2024-11-14, published in March 2025.

to fulfil the accuracy and efficiency criteria. The collaborative traceability of multiple UAVs has become the key to solving this problem, which centres on using swarm intelligence algorithms. These algorithms originate from group behaviour in the biological population and find the optimal path to solve the problem through sharing experiences and cooperation between individuals. In the field of gas traceability, the commonly used swarm intelligence algorithms include particle swarm optimization algorithm (PSO) [10], ant colony optimization algorithm (ACO) [11], and genetic algorithm (GA) [12]. Van [13] designed an algorithm that fully uses the very compassionate characteristics of the fruit fly olfactory system. The algorithm designs corresponding decision strategies according to different search stages so fruit flies can explore the environment widely in the early stage and gradually turn to more likely areas for in-depth search. With the help of swarm intelligence algorithms and active olfaction, multi-UAVs have better collaborative traceability and optimize search paths to improve the accuracy and efficiency of traceability results.

In this study, a swarm intelligence algorithm based on the basic Jaya algorithm is proposed to solve the collaborative traceability task of multiple UAVs. It innovatively combines psychological theories to apply human psychological states to the traceability tasks of UAVs. By utilizing a combination of various UAV and swarm intelligence optimization algorithms, gas sources can be searched more accurately. This method greatly enhances the information perception and environment recognition capabilities of UAVs, significantly reducing the search time and improving the overall traceability efficiency.

2. DESIGN OF THE EIJAYA GAS TRACEABILITY ALGORITHM

Aiming at the problems in the basic Jaya algorithm, this paper proposes an improved version based on emotional intelligence, abbreviated as EIJaya. The improved algorithm mainly introduces self-evaluation and social evaluation based on the traditional algorithm to improve its convergence speed and optimization ability. It increases the attention to the individual state of the UAV to achieve a more accurate and more efficient traceability effect.

2.1. Basic Jaya algorithm

The basic Jaya algorithm is a meta-heuristic optimization algorithm proposed by scholar Rao [14] in 2016. The algorithm is known for its simple and efficient features without specific control parameters. The Jaya algorithm realizes cooperation and competition among individuals through a cooperation mechanism, which promotes the evolution of excellent individuals to better solutions and avoids the adverse effects of inferior individuals on the whole. Through this cooperation, individuals can communicate and learn from each other to obtain better solutions. At the same time, the competition mechanism between individuals also plays a role in screening excellent solutions and eliminating inferior solutions so that the population can gradually converge to the global optimal solution. The position update formula is shown in (1):

$$X_{i+1} = X_i + r_1 \left(X_{\text{best}} - |X_i|\right) - r_2 \left(X_{\text{worst}} - |X_i|\right), \tag{1}$$

where X_i is the current search position of the UAV, X_{i+1} is the updated search position of the UAV, X_{best} is the location of the UAV with the highest gas concentration searched, X_{worst} is the location of the UAV with the lowest gas concentration searched, and r_1, r_2 are random numbers between $[0,1]$.

As the algorithm converges faster, it may reduce the diversity of the population, trapping the population in a region of local optimality and affecting the global optimization capability [15]. At the same time, the Jaya algorithm is limited by the absolute value sign when dealing with optimization problems in positive search space, which will affect its efficiency. Therefore, to effectively apply the Jaya algorithm to solve various optimization problems and enhance the convergence speed, the global search ability, and the stability and robustness of the algorithm, it needs to be improved to be more effective in addressing the flue gas traceability problem.

2.2. EIJaya algorithm design

2.2.1. Self-evaluation and social evaluation

Self-evaluation is an important psychological concept that reflects an individual's perception and assessment of his or her abilities and values. Psychology-related studies have shown that people with higher levels of self-evaluation are more confident in their abilities [16]. Similarly, self-evaluation helps UAVs decide on their next course of action. In the two-dimensional self-evaluation model, the X-axis indicates the UAV detected distance from its teammates. When the UAV is farther away from its teammates, it is more confident and decisively executes commands to complete the search task to the best of its ability.

Conversely, when the UAV is closer to its teammates, it tends to reduce its stride length or withdraw to avoid a collision. The Y-axis indicates the UAV electricity status. The UAV can execute the corresponding task when its electricity is high, while the UAV will be more easily exhausted when the battery is low and will have some difficulties in perfroming the following search task. In this self-evaluation two-dimensional model, the rules for determining each coordinate value are shown in equations (2) and (3):

$$a_i = \frac{n - w_i}{n}, \tag{2}$$

$$b_i = \frac{Q_i}{100}, \tag{3}$$

where a_i is the value of the X-axis of the self-evaluation 2D model, b_i is the value of the Y-axis of the self-evaluation 2D model, n is the population size, i.e., the number of UAVs, w_i is the number of UAVs i spaced from other teammates beyond the safe distance $d_{\min}$, and Q_i is the percentage of UAV battery.

Based on the values of the X-axis and Y-axis in the self-evaluation model, the self-evaluation factor $P_{\text{self},i}$, of the UAV can be calculated using equation (4):

$$P_{\text{self},i} = \sqrt{\frac{a_i^2 + b_i^2}{2}}\,. \tag{4}$$

At this time, the drone has preliminary anthropomorphic emotion, and on this basis, it more accurately reflects the emotional condition of the drone by imitating the idea of social evaluation in the social-emotional optimization algorithm [17]. The UAV is divided into three categories: clumsy, ordinary, and sensitive individuals, using the social-evaluation rules. The following evolutionary behaviour is chosen based on the individual's emotional condition, which improves with higher social assessment. The following are the social evaluation guidelines:

$$\begin{cases} \text{clumsy individuals}, & c_i < c_{\text{mean}}\,, \\ \text{ordinary individuals}, & c_{\text{mean}} \le c_i \le c_{\text{gmean}}\,, \\ \text{sensitive individuals}, & c_{\text{gmean}} < c_i\,, \end{cases} \tag{5}$$

$$c_{\text{mean}} = \frac{1}{n}\sum_{i=1}^{n} c_i\,, \tag{6}$$

where c_i is the value of gas concentration searched by UAV i at the current location, and the average gas concentration searched by the UAV swarm is c_{mean}. Individuals with concentration values higher than the average concentration are categorized as high-quality individuals and the average concentration of the high-quality individuals is calculated and noted as c_{gmean}.

The social-evaluation factor $\mathrm{P}_{social,i}$ of UAVs is calculated as shown in equation (7):

$$P_{\text{social},i} = \frac{c_i}{c_{\max}}\,, \tag{7}$$

where $c_{\max}$ is the highest gas concentration value searched in the UAV swarm.

2.2.2. Position update formula optimization

In the basic Jaya algorithm, random numbers are used in the position-updating rules, and social evaluation factors and self-evaluation factors are introduced in the position-updating rules. By assessing the UAV state, its subsequent behaviour is more evidence-based, and the UAV should update its position according to the revised rules for different individuals.

When the concentration detected by the UAV is lower than the overall average concentration, it proves that the clumsy individual is not highly effective in searching at the current location, and it is necessary to expand the search space of the individual. The positional update equation is as follows:

$$\begin{aligned} X_{i+1} = X_i &+ \left(\frac{p_{\text{social},i} + r_1}{2}\right) \times (X_{\text{best}} - |X_i|) \\ &- \left(\frac{p_{\text{self},i} + r_2}{2}\right) \times (X_{\text{worst}} - |X_i|)\,. \end{aligned} \tag{8}$$

When the concentration detected by the UAV is higher than the overall average concentration but lower than the average concentration of high-quality individuals, it indicates that the search of ordinary individuals at the current location is effective. However, it still needs to be improved. As the number of iterations increases, most individuals will gather around the current optimal individual for local search. In contrast, the other few lagging individuals will move away from the current optimal individual to perform the global exploration task. During this search process, the average position of the current population shifts. Therefore, the mean value of the current position is introduced into the position update rule of ordinary individuals so that the algorithm can escape from the local optimum, resulting in improved search performance of the population. The positional update equation is as follows:

$$\begin{aligned} X_{i+1} = X_i &+ \left(\frac{p_{\text{social},i} + r_1}{2}\right) \times (X_{\text{best}} - |X_i|) \\ &- \left(\frac{p_{\text{self},i} + r_2}{2}\right) \times (X_{\text{mean}} - |X_i|)\,, \end{aligned} \tag{9}$$

$$X_{\text{mean}} = \frac{1}{n}\sum_{i=1}^{n} X_i\,, \tag{10}$$

where X_{mean} is the average position of the UAV population.

When the concentration detected by the UAV is higher than the average concentration of high-quality individuals, the search of the machine-sensitive individuals at the current position is amazingly effective. The current optimal individual is the dominant one in the UAV swarm, which is oriented to the current optimal individual to accelerate the convergence of the Jaya algorithm. A random perturbation term is added to the position-updating rule of the machine-sensitive individuals, i.e., by randomly selecting two UAVs to utilize their current position to avoid the situation that the second term of the formula is 0 and cannot update the position when the current individual is the optimal individual, and its position update formula:

$$\begin{aligned} X_{i+1} = X_i &+ \left(\frac{p_{\text{social},i} + r_1}{2}\right) \times (X_{\text{best}} - |X_i|) \\ &+ \left(\frac{p_{\text{self},i} + r_2}{2}\right) \times (X_l - X_m)\,, \end{aligned} \tag{11}$$

where l, m are random integers between $[1, n]$ and l, m are not equal to i.

2.2.3. EIJaya algorithm flow

The specific steps of the EIJaya algorithm for gas source localization are as follows:

Step 1: Initialize settings, including the number of UAVs n, the initial position of each UAV, and the maximum number of iterations.

Step 2: Based on the internal state of each UAV, establish a two-dimensional self-assessment model and calculate the self-assessment factor.

Step 3: Classify the UAVs into three categories based on the social evaluation rules according to the gas concentrations detected by each UAV and calculate the social evaluation factor.

Step 4: Incorporate the self-assessment factor and social evaluation factor into the position update rules and update the positions and the detected gas concentrations according to the corresponding rules for each individual.

Step 5: Check if the maximum number of iterations has been reached. If it has, proceed to Step 6; if not, increase the iteration count by 1 and return to Step 2.
Step 6: Output the position with the highest gas concentration, and the algorithm ends.

The overall flow of the EIJaya algorithm for gas source localization is illustrated in Fig. 1.

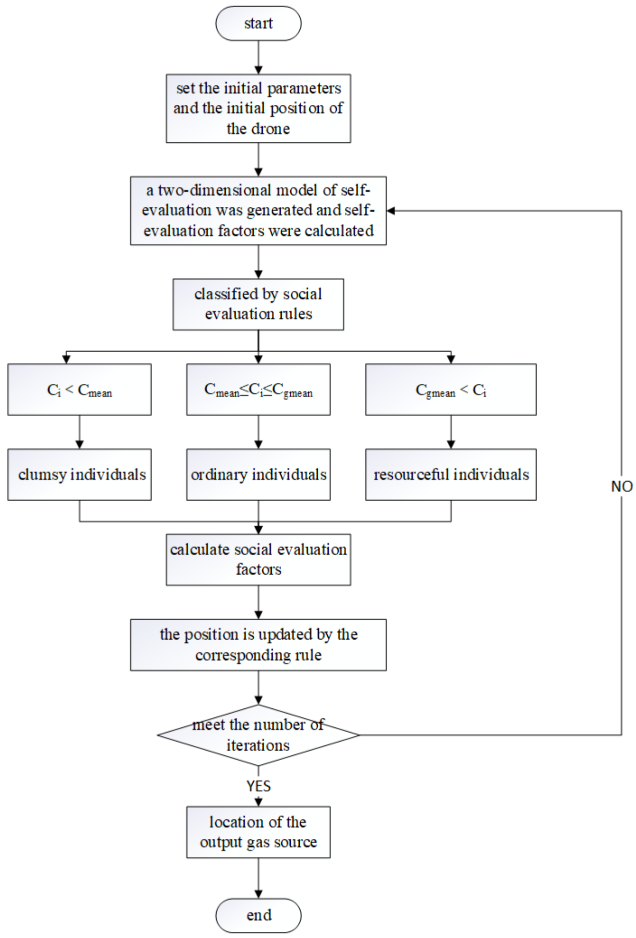

Fig. 1. Flowchart of the traceability of the EIJaya algorithm

3. EXPERIMENTAL VALIDATION OF EIJAYA GAS TRACEABILITY ALGORITHM IN SIMULATION

To evaluate the performance stability and adaptability of the algorithm, considering that it is impossible to control the changes of all factors in the natural environment, it is necessary to set different environmental parameters, such as wind speed and source strength, to simulate such changes. By changing the wind speed and source strength, multiple simulated concentration fields can be constructed to simulate the gas diffusion in different scenarios, which can effectively evaluate the robustness and reliability of the algorithm. In this paper, five different wind speeds are selected, which are 0.5 m/s, 2.0 m/s, 4.0 m/s, 6.0 m/s, and 8.0 m/s, and five different source strengths are set, which are 0.002kg/s, 0.004kg/s, 0.006 kg/s, 0.008 kg/s, and 0.010 kg/s. To make an objective and comprehensive algorithmic evaluation, this paper chooses success rate, iteration times, and distance ratio as performance evaluation indexes. The distance ratio is a measure of the energy efficiency of the algorithm by calculating the ratio of the total distance by the UAV to the straight-line distance from the starting point to the final point. The closer the ratio is to 1, the better the algorithm performance is. The Jaya algorithm, PSO algorithm, and EIJaya algorithm are run 200 times in each different turbulent concentration field, and the success rate is represented by a line graph. The iteration times and the distance ratio are shown using a half-violin plot.

3.1. Analysis of the effect of wind speed on algorithm performance

Based on Fig. 2, it can be seen that the EIJaya algorithm performs well in terms of success rate in the environment of changing wind speed, which is significantly better than the Jaya algorithm and PSO algorithm. In five different wind speed environments, the average success rate of the EIJaya algorithm reaches 92.9%, which is higher than that of the Jaya algorithm at 77.6% and that of the PSO algorithm at 49.6%.

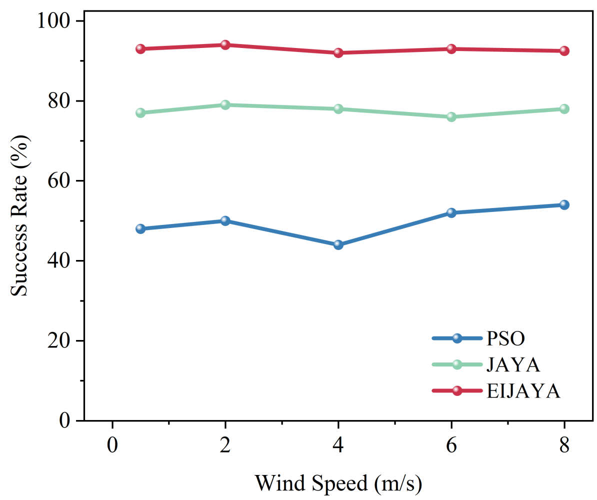

Fig. 2. Effect of wind speed variations on success rates

Based on Fig. 3, it can be seen that the change in wind speed affects the distance ratio and the iteration times of the three algorithms. Regarding the distance ratio, the average distance ratio of the PSO algorithm and the EIJaya algorithm basically stays below 3.0 under different wind speeds, which outperforms the Jaya algorithm. The data of the Jaya algorithm is distributed in the interval of $[2.0, 4.0]$ as a whole; the overall distribution of the PSO algorithm fluctuates under different wind speeds and is roughly distributed in the range of $[1.5, 3.5]$. Most of the data of the EIJaya algorithm is distributed in the range of $[1.0, 3.0]$, with only a tiny portion distributed between $[3.0, 6.0]$. In contrast, with the change in wind speed, the distance ratio by the Jaya algorithm and the EIJaya algorithm is more stable than that of the PSO algorithm, showing better robustness. In terms of the iteration times, the average iteration number of the EIJaya algorithm for successful traceability under the five different wind speed environments is around 21, which is much less than that

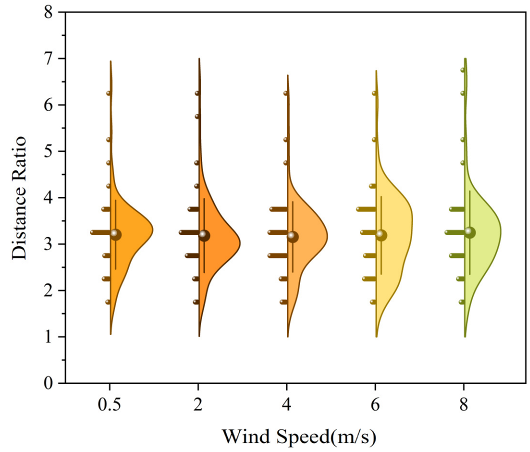

(a) Impact on the distance ratio of the Jaya algorithm

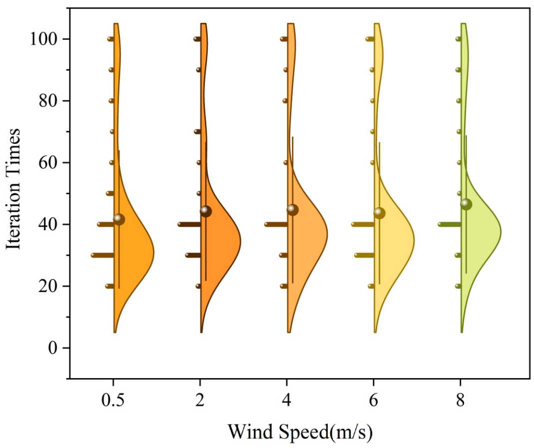

(b) Impact on the iteration times of the Jaya algorithm

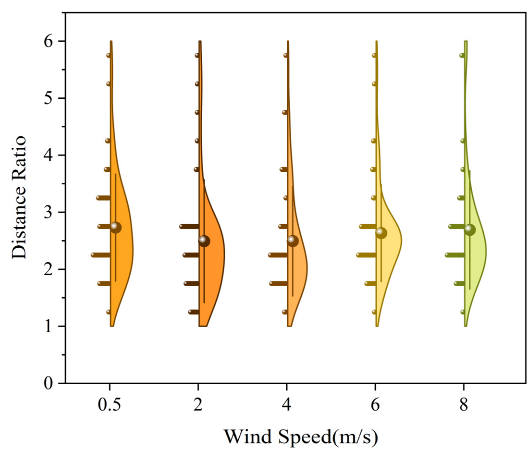

(c) Impact on the distance ratio of the PSO algorithm

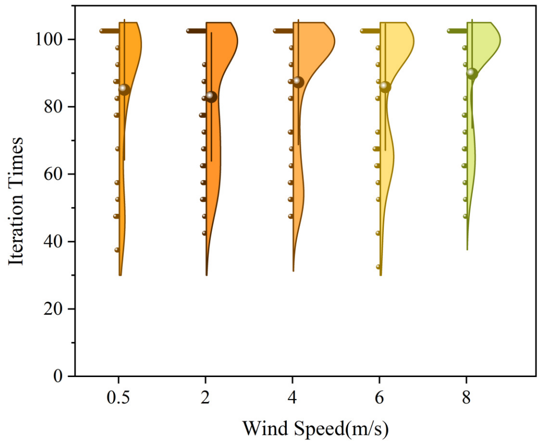

(d) Impact on the iteration times of the PSO algorithm

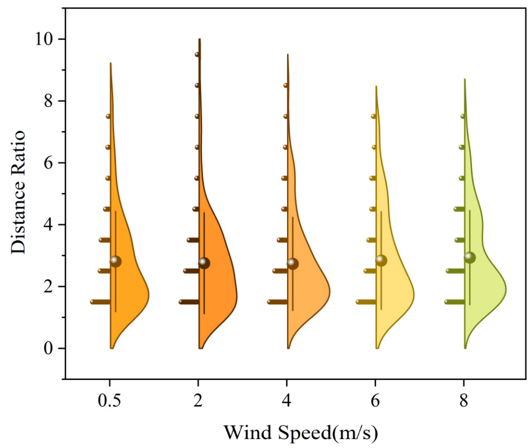

(e) Impact on the distance ratio of the EIJaya algorithm

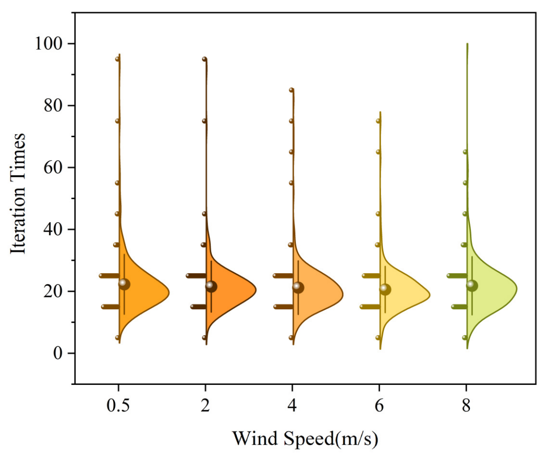

(f) Impact on the iteration times of the EIJaya algorithm

Fig. 3. Effect of wind speed variation on distance ratio and iteration times

of the PSO algorithm and slightly higher than that of the Jaya algorithm. With the gradual increase of wind speed, the iteration number of the PSO algorithm shows a fluctuating upward trend, and most of the data are distributed above 80 times. In contrast, the distribution state of the iteration number of the Jaya algorithm and EIJaya algorithm remains unchanged. The average iteration number of the Jaya algorithm slightly increases, exceeding 40, whereas the EIJaya algorithm exhibits a more centralized distribution, mainly within the range of 13 to 30, with better performance.

3.2. Analysis of the impact of source strength on algorithm performance

As shown in Fig. 4, the success rates of the three algorithms fluctuate slightly in different source strength environments, with the EIJaya algorithm having a significantly higher success rate than the Jaya algorithm and the PSO algorithm. In the five simulation environments with different source strengths, the average success rate of the EIJaya algorithm reaches 91.7%, while that of the Jaya algorithm is 82.3%, and that of the PSO algorithm is only 47%.

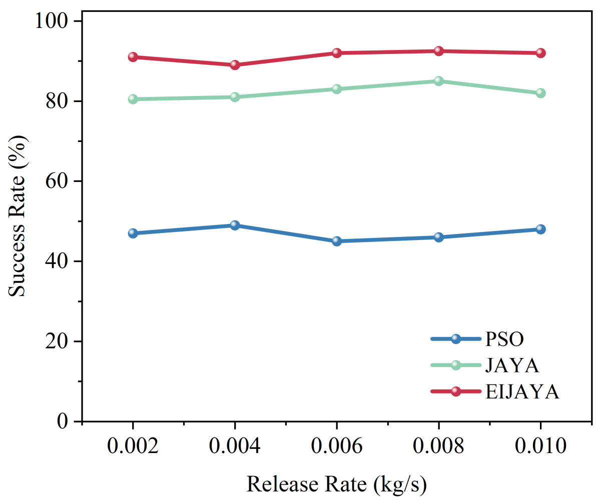

Fig. 4. Effect of release rate variation on success rate

Under different release rate environments, the changing trend of the distance ratio and the iteration times of the three algorithms is shown in Fig. 5. The PSO algorithm performs well in the average distance ratio. With the release rate increase, the average distance ratio decreases slightly from about 2.5 to about 2.3, and the data are mainly distributed in the interval of $[1.5, 3.5]$. The distance ratio of the Jaya algorithm shows a slight upward trend with the increase in release rate, and the average distance ratio reaches 3.5 when the release rate is 0.01 kg/s and the data greater than 6.0 increases. The average distance ratio of the EIJaya algorithm is about 2.7, which is more stable than that of the PSO algorithm and the Jaya algorithm. The data are mainly distributed in the interval of $[1.0, 3.0]$. A small portion of the data is distributed in the interval of $[3.0, 6.0]$. In terms of the iteration times, the EIJaya algorithm performs well; the average number of iterations is about 33 times without obvi-

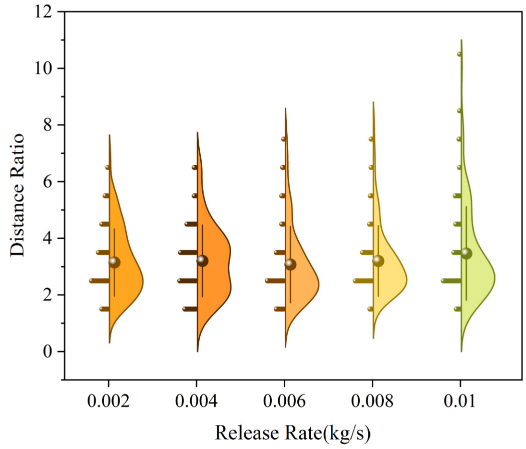

(a) Impact on the distance ratio of the Jaya algorithm

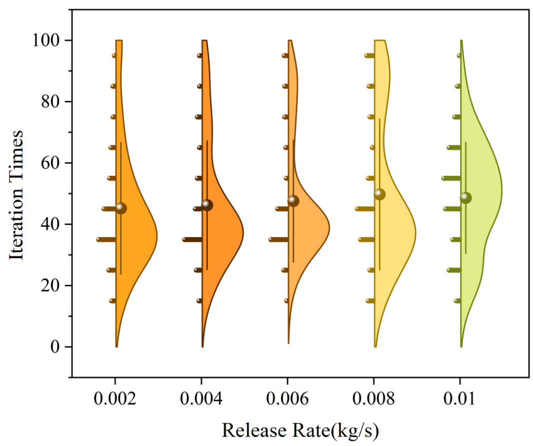

(b) Impact on the iteration times of the Jaya algorithm

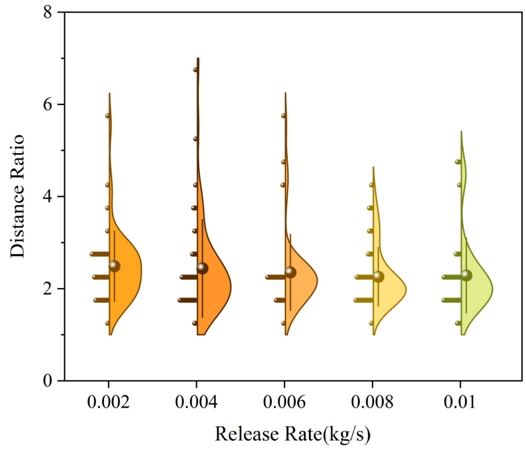

(c) Impact on the distance ratio of the PSO algorithm

Fig. 5

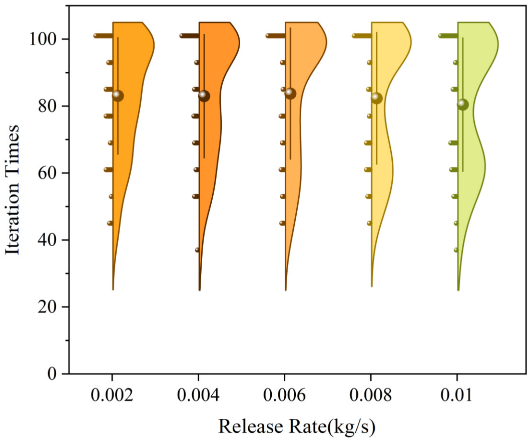

(d) Impact on the iteration times of the PSO algorithm

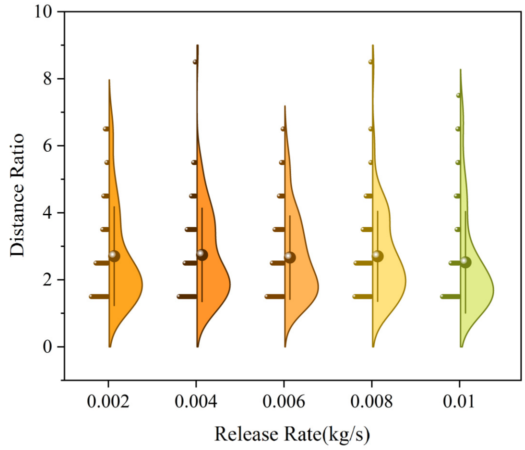

(e) Impact on the distance ratio of the EIJaya algorithm

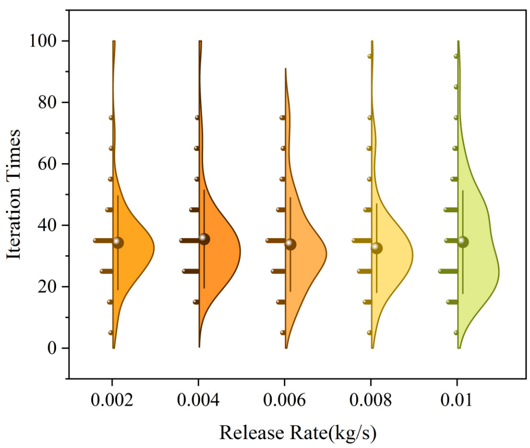

(f) Impact on the iteration times of the EIJaya algorithm

Fig. 5. Effect of release rate variation on distance ratio and iteration times

ous fluctuations, and the data distribution is more concentrated, basically below 60 times. The average number of iterations of the Jaya algorithm shows an upward trend. The data above 50 times gradually increase, and the data are slightly dispersed. The average number of iterations of the PSO algorithm fluctuates slightly. As the source strength increases, the data below 75 times gradually increase, but the average number of iterations remains above 80 times.

3.3. Analysis of the effect of the number of UAVs on the performance of the algorithm

The change in the success rate of the three algorithms when the number of UAVs is gradually increased from 3 to 8 is shown in Fig. 6. The EIJaya algorithm performs slightly worse than the PSO algorithm and the Jaya algorithm when the number of drones is 3 and 4. However, when the number of drones increases to 5, the success rate of the EIJaya algorithm shows a significant increase and reaches 90.5% at the number of 6 drones. In contrast, the Jaya algorithm, despite some degree of improvement, has a maximum success rate of only 81%, while the PSO algorithm has an optimal success rate of only 66%.

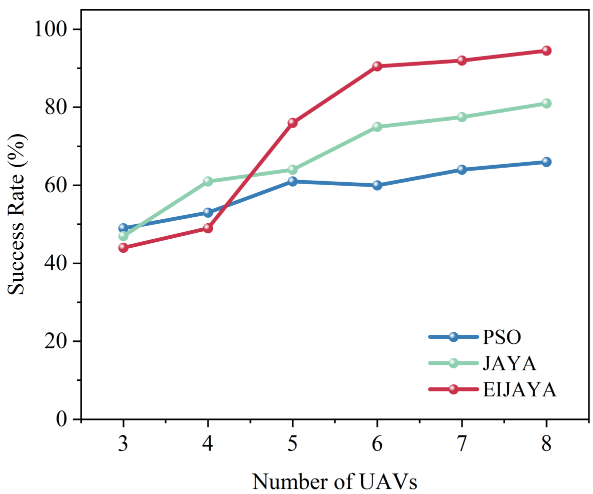

Fig. 6. Impact of changes in the number of UAVs on success rates

According to the results shown in Fig. 7, it can be seen that the change in the number of UAVs has an impact on the distance ratio and the iteration times of the three algorithms. As far as the distance ratio is concerned, all three algorithms show an increasing trend. The PSO algorithm performs the best, the data distribution is more centralized, and when the number of drones reaches 5, the average distance ratio stays around 2.9. The average distance ratio of the Jaya algorithm shows a fluctuating growth overall, staying above 3.0 when there are 6 to 8 drones and reaching 3.5 when there are 7 drones, and the main data distribution area also shows an upward trend; the data below 2.5 will increase first and then decrease with the increase of the number of drones. The average distance ratio of the EIJaya algorithm is more concentrated, and the overall average distance ratio performs better, with an average distance ratio of about 2.4 for 3 and 4 drones and an average distance ratio of about 2.7 for 5

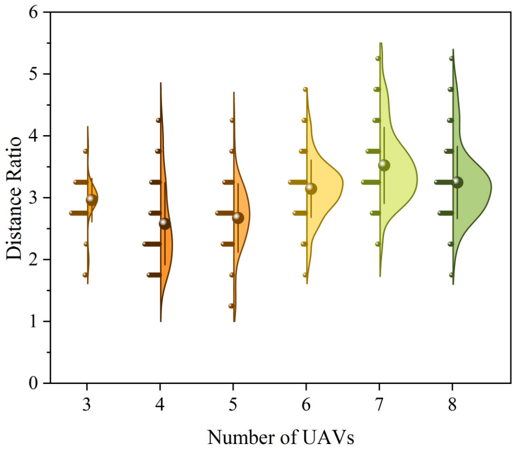

(a) Impact on the distance ratio of the Jaya algorithm

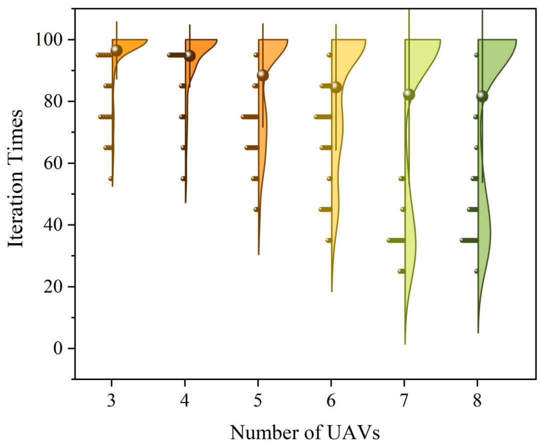

(d) Impact on the iteration times of the PSO algorithm

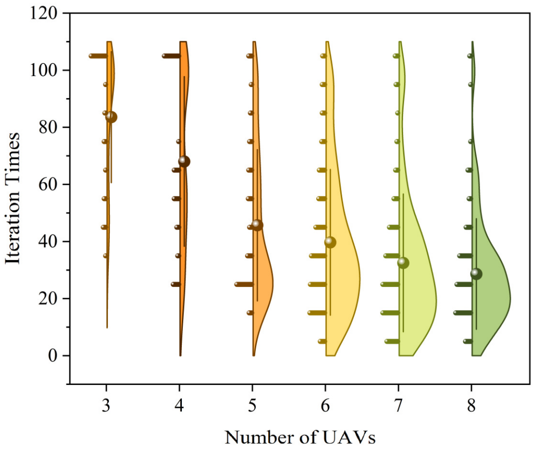

(b) Impact on the iteration times of the Jaya algorithm

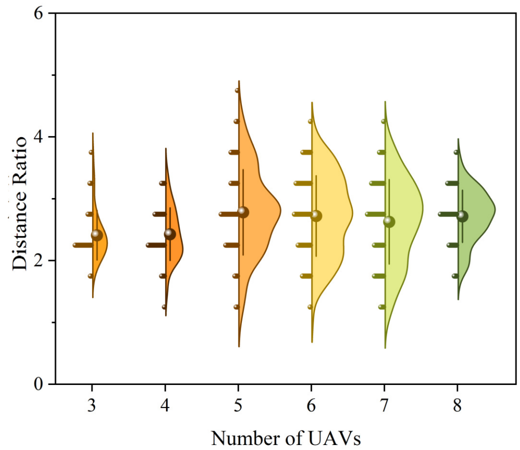

(e) Impact on the distance ratio of the EIJaya algorithm

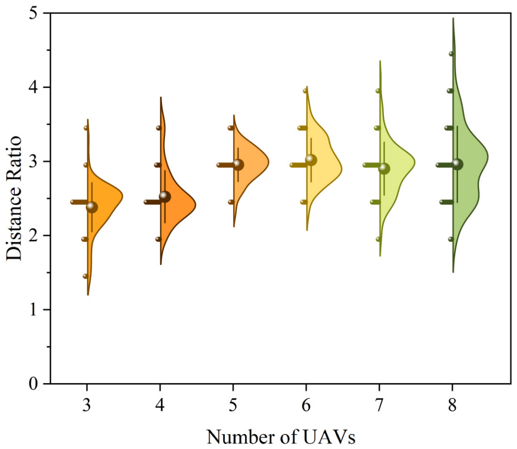

(c) Impact on the distance ratio of the PSO algorithm

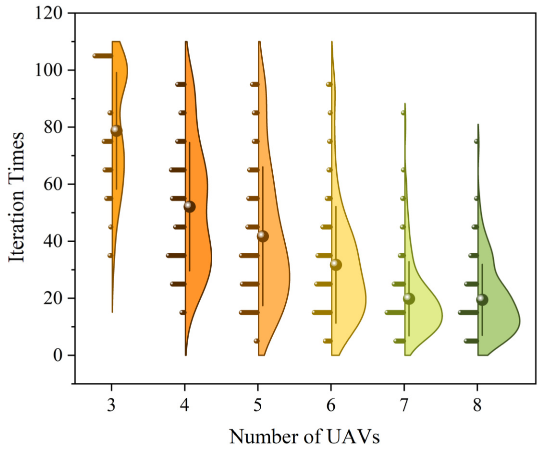

(f) Impact on the iteration times of the EIJaya algorithm

Fig. 7. Effect of number of UAVs on distance ratio and iteration times

to 8 drones. Regarding the number of iterations, as the number of UAVs increases, the number of iterations required for successful localization of all three algorithms shows a decreasing trend. Although all of them have improved their performance, the Jaya algorithm still has more data over 60 times, and the PSO algorithm still occupies the majority of data over 80 times. In contrast, the EIJaya algorithm has a gradual increase in the amount of data under 40 times and a gradual decrease in the number of data over 80 times. Regarding the average number of iterations, the EIJaya algorithm performs the best, much less than the PSO algorithm and slightly less than the Jaya algorithm. Still, the performance improvement is not apparent when the number of drones increases from 7 to 8. Therefore, it is sufficient to use 6 UAVs, and there is no need to allocate more UAVs to increase the cost.

By comprehensively analyzing the performance of the three algorithms under different wind speeds, release rates, and numbers of UAVs, it is evident that the EIJaya algorithm outperforms others in terms of success rate and iteration times. It is slightly inferior to the PSO algorithm regarding the average distance ratio but still better than the Jaya algorithm. Wind speed and release rate do not significantly impact the EIJaya algorithm, indicating that it is robust. The change in the number of drones has a more significant effect on the EIJaya algorithm, and the increase in the number of drones later causes an increase in the distance ratio, probably because the contractual collaborative traceability between the drones increases the distance travelled.

4. EXPERIMENTAL VALIDATION OF THE EIJAYA GAS TRACEABILITY ALGORITHM

4.1. Construction of experimental hardware system

The DJI RoboMaster Tello Talent (TT) UAV was chosen for this experiment, and the TT UAV consists of two parts: the flight vehicle and the expansion accessories. The vehicle contains components such as flight control, communication system, visual positioning system, power system, and flight battery, which provide functions such as stable flight, positioning, and power output. Expansion accessories can be added to the aircraft to realize a broader function expansion and programming environment, promote multi-aircraft cooperative control, and write diverse formation control programs.

Specifically, the visual localization system of the TT UAV, which consists of a camera and an infrared sensor, is located at the bottom. This visual positioning system uses a combination of images and infrared sensors to obtain the position information of the vehicle using the camera and determine the current altitude through the infrared sensors to realize the precise positioning of the vehicle and to provide a reference of the vehicle altitude to the ground. The extension module part of the TT UAV is an open-source controller built-in with an ESP32 chip, which integrates a dual-frequency WiFi module and a Bluetooth module. It supports graphical programming, Python, and other programming languages to write multi-copter cooperative flight programs. Serial communication is realized through the UAV onboard Micro USB interface, providing power to the TT expansion modules. This enables multiple RoboMaster TT UAVs to be connected to a WiFi router simultaneously to achieve multi-machine state synchronization and cooperative control, and its specific control mode is shown in Fig. 8.

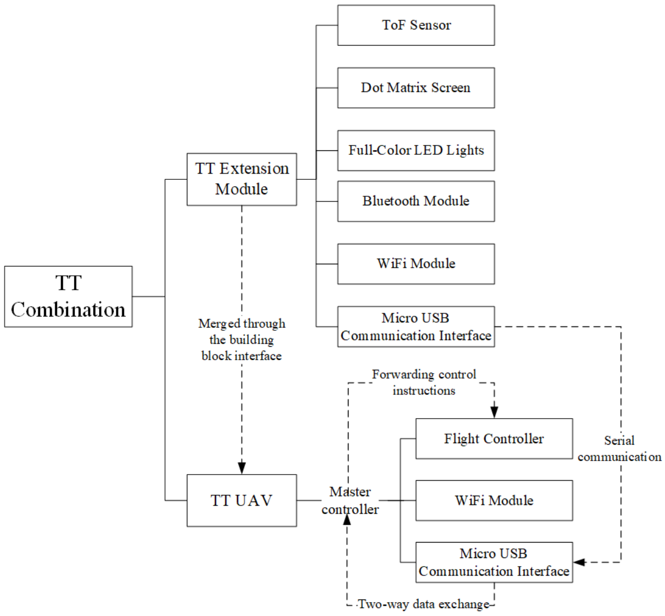

Fig. 8. TT combination control mode

The expansion board used in this study provides interfaces to connect the signal pins of the ESP32 and the GND, 5V, and 3.3V power supplies to the ESP32 expansion module, which facilitates the integration of other open-source hardware and third-party sensors into the system for gas traceability. Figure 9 shows the specific control of the UAV.

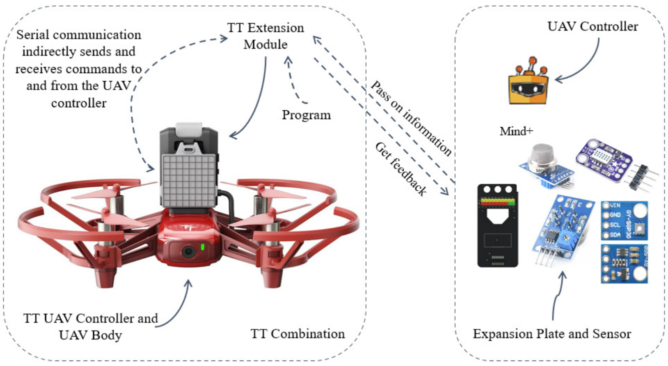

Fig. 9. UAV control mode

4.2. Experimental scenario construction

To simulate a relatively stable gas diffusion scenario and better control the experimental conditions, this experiment used a metal steel frame and plastic film to construct a transparent closed three-dimensional space (see Fig. 10). The specific dimensions of this experimental space are 3 m in length, 3 m in width, and 1.8 m in height. CO_2 in the fire signature gas is a non-toxic gas, and to ensure the safety of the experiment, food-grade CO_2 cylinders with a purity of ≥ 99.9% were selected as the gas source for this indoor traceability experiment. In order to accurately control the amount of CO_2 released, the flow rate of the gas was controlled by installing a pressure reducer, as shown in Fig. 11. In addition, an air inlet with a specification of 20 cm × 20 cm was opened at the rear side film 100 cm from the ground, and a fan was used to provide a constant wind speed for the experiment to ensure that the CO_2 was fully diffused in the experimental space, as shown in Fig. 12.

Fig. 10. Indoor lab space map

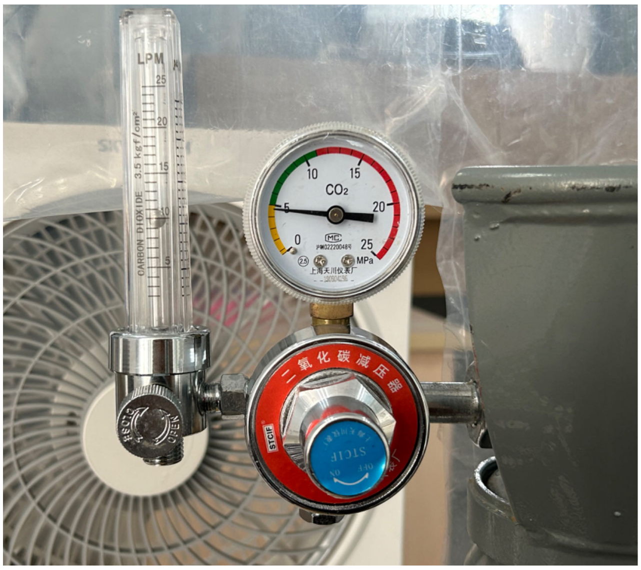

Fig. 11. CO_2 pressure reducing valve

In this study, CO_2 was detected using the SGP30 sensor, as shown in Fig. 13. The SGP30 is an electrochemical-based sensor with an internal metal oxide sensing element that is heated and reacts with chemicals in the air, resulting in a change in the conductance of the aspect, generating an electrical signal to measure and quantitatively analyze the concentration of CO_2 in the air. The SGP30 is easily integrated into a mobile device

Fig. 12. Fans and emission sources

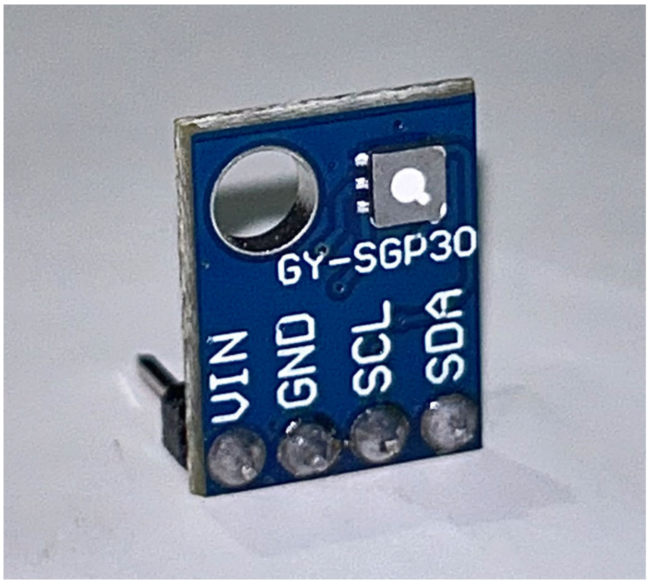

Fig. 13. SGP30 sensor

with 12 × 12 × 1.6 mm dimensions and is suitable for TT drones. The sensor-equipped UAV utilizes a flight map for localization, where the position is determined by recognizing signs and patterns on the map with a vision sensor. The flight map shown in Fig. 14 is a 3 m × 3 m area containing the DJI Logo, decorative pattern, and a small planet. The DJI Logo represents the positive direction of the X-axis, and the centre is the origin of the coordinate system. The small planet pattern identifies the map and obtains the coordinates. The map should be placed horizontally, and the logo should be oriented so the UAV can recognize the logo and record its position with Mind+ programming. Figure 15 shows a schematic of the coordinates corresponding to the flight map, where the CO_2 emission source is set at $(0, 140)$, and the unit is cm.

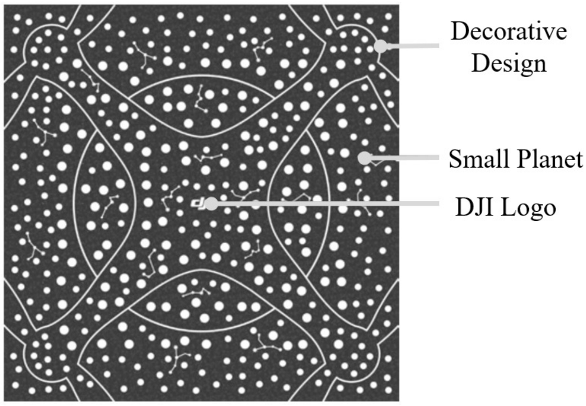

Fig. 14. Flight map

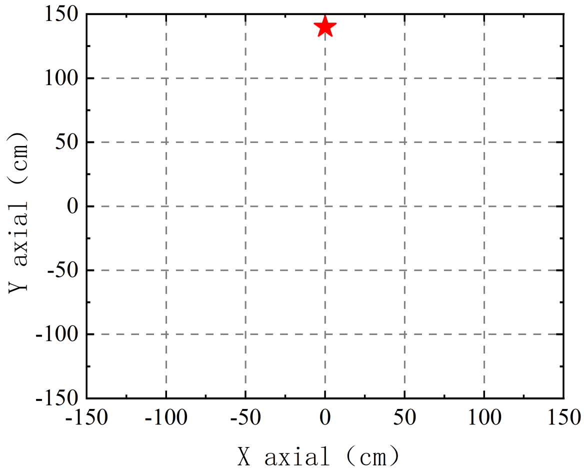

Fig. 15. Map coordinates of indoor experiment

4.3. Results showcase

For indoor traceability experiments, the CO_2 cylinder needs to be opened, and the pressure-reducing valve adjusted to 5 MPa, 3.5 kgf/cm^2, to ensure that the CO_2 is released at a constant flow rate. At the same time, the fan was turned on to promote the complete diffusion of CO_2 throughout the experimental area. After five minutes, three UAVs were randomly placed in the experimental area with initial position coordinates of $(46, -18)$, $(-39, -95)$, and $(-116, 77)$, respectively, and the UAVs were kept at the same altitude during flight, as shown in Fig. 16a. Figure 16b shows the flight trajectories of the three UAVs in the traceability experiment, and each UAV works together to complete the traceability task by mutually cooperating. In the initial stage of the experiment, UAV No. 3 is a resourceful individual, so UAVs No. 1 and No. 2 tend to be closer to UAV No. 3 for a better traceability task. After exchanging information with each other and being conditioned by the emotionally intelligent Jaya algorithm, the three drones gradually converged to search in the same direction. Eventually, they are located at $(0, 133)$, $(-4, 118)$, and $(7, 122)$, respectively. The straight-line distance between the UAV closest to the emission source and the source was 7 cm, and the entire process of the traceability experiment took a total of 47 seconds.

(a) UAV flight process

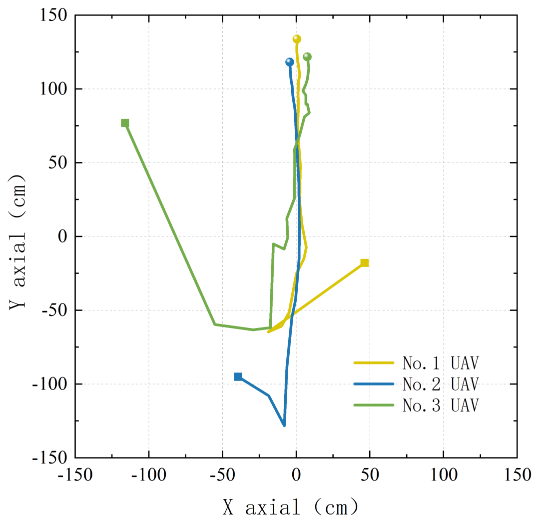

(b) UAV flight trajectory

Fig. 16. Indoor traceability experiment

The experimental results show that the emotionally intelligent Jaya algorithm proposed in this paper is feasible in indoor traceability experiments and can successfully locate the source of CO_2 emissions.

5. CONCLUSIONS

Focused on the defect of the basic Jaya algorithm easily falling into the local optimum in the multi-UAV cooperative traceability task, this study innovatively combines the psychological theory, applies the human psychological state to the traceability task of the UAV, and proposes the EIJaya algorithm. The EIJaya algorithm assigns self-evaluation and social evaluation to the UAV so that it can make more intelligent decisions according to its state and surrounding environment, increases the population diversity, improves the position update formula, avoids the local optimal problem caused by a single strategy, and improves the convergence speed and optimization ability of the algorithm. In the constructed concentration field, several different simulated concentration fields were generated by changing the wind speed and source strength of the environmental conditions, and experimental assessment was conducted using different numbers of UAVs. The evaluation was conducted by selecting three indexes. Namely, success rate, iteration number, and distance travelled ratio, as well as comparing and evaluating the basic Jaya and particle swarm algorithms. The results show that the EIJaya algorithm performs better in the multi-UAV cooperative traceability task. When improving the emotionally intelligent Jaya algorithm in the future, it is necessary to consider the three-dimensional characteristics of smoke diffusion and include the obstacle avoidance function when the UAV is flying. This will enable the algorithm to better cope with the challenges in real-life scenarios, improve the accuracy and applicability of gas identification, and apply it to a broader range of scenarios.

ACKNOWLEDGEMENTS

This study was supported by Zhejiang Provincial Administration for Market Regulation "Young Eagle Plan" cultivation project (No. CY2023003), Zhejiang Provincial Administration for Market Regulation (No. 2022MK058), Public Welfare Science and Technology Program Projects of Ningbo Science and Technology Bureau (No. 2022S121).

REFERENCES

[1] S. Loganathan and J. Arumugam, "Clustering algorithms for wireless sensor networks survey," *Sensor Lett.*, vol. 18, no. 2, pp. 143–149, 2020, doi: 10.1166/sl.2020.4193.

[2] K. Langer, "A guide to sensor design for land mine detection," in *EUREL International Conference The Detection of Abandoned Land Mines: A Humanitarian Imperative Seeking a Technical Solution* (Conf. Publ. No. 431), IET, 1996, pp. 30–32, doi: 10.1049/cp:19961073.

[3] A.J. Bell, "Like moths to a flame: A review of what we know about pyrophilic insects," *Forest Ecol Manage.*, vol. 528, p. 120629, 2023, doi: 10.1016/j.foreco.2022.120629.

[4] R. Rozas, J. Morales, and D. Vega, "Artificial smell detection for robotic navigation," in *Fifth International Conference on Advanced Robotics' Robots in Unstructured Environments*, IEEE, 1991, pp. 1730–1733, doi: 10.1109/icar.1991.240354.

[5] V. Genovese, P. Dario, R. Magni, and L. Odetti, "Self organizing behavior and swarm intelligence in a pack of mobile miniature robots in search of pollutants," in *Proceedings of the IEEE/RSJ international conference on intelligent robots and systems*, IEEE, 1992, vol. 3, pp. 1575–1582, doi: 10.1109/iros.1992.594225.

[6] Z. Fu, Y. Chen, Y. Ding, and D. He, "Pollution source localization based on multi-UAV cooperative communication," *IEEE Access*, vol. 7, pp. 29304–29312, 2019, doi: 10.1109/access.2019.2900475.

[7] L. Heimsch *et al.*,"Carbon dioxide fluxes and carbon balance of an agricultural grassland in southern Finland," *Biogeosciences*, vol. 18, no. 11, pp. 3467–3483, 2021, doi: 10.5194/bg-18-3467-2021.

[8] L. Carlier, I. Rotar, M. Vlahova, and R. Vidican, "Importance and functions of grasslands," *Notulae Botanicae Horti Agrobotanici Cluj-Napoca*, vol. 37, no. 1, pp. 25–30, 2009, doi: 10.15835/nbha3713090.

[9] H. Liu, L. Hou, N. Kang, Z. Nan, and J. Huang, "The economic value of grassland ecosystem services: A global meta-analysis," *Grassland Res.*, vol. 1, no. 1, pp. 63–74, 2022, doi: 10.1002/glr2.12012.

[10] O.F. Aje and A.A. Josephat, "The particle swarm optimization (PSO) algorithm application – A review," *Glob. J. Eng. Technol. Adv.*, vol. 3, no. 3, pp. 001–006, 2020, doi: 10.30574/gjeta.2020.3.3.0033.

[11] H. Sheng *et al.*, "An advanced gas leakage traceability & dispersion prediction methodology using unmanned aerial vehicle," *J. Loss Prev. Process Ind.*, vol. 88, p. 105276, 2024, doi: 10.1016/j.jlp.2024.105276.

[12] Y. Liu, Y. Jiang, X. Zhang, Y. Pan, and Y. Qi, "Combined grey wolf optimizer algorithm and corrected Gaussian diffusion model in source term estimation," *Processes*, vol. 10, no. 7, p. 1238, 2022, doi: 10.3390/pr10071238.

[13] F. van Breugel, "Correlated decision making across multiple phases of olfactory-guided search in Drosophila improves search efficiency," *J. Exp. Biol.*, vol. 224, no. 16, p. 242267, 2021, doi: 10.1242/jeb.242267.

[14] R. Rao, "Jaya: A simple and new optimization algorithm for solving constrained and unconstrained optimization problems," *Int. J. Ind. Eng. Comput.*, vol. 7, no. 1, pp. 19–34, 2016, doi: 10.5267/j.ijiec.2015.8.004.

[15] K. Yu, J. Liang, B. Qu, X. Chen, and H. Wang, "Parameters identification of photovoltaic models using an improved JAYA optimization algorithm," *Energy Conv. Manage.*, vol. 150, pp. 742–753, 2017, doi: 10.1016/j.enconman.2017.08.063.

[16] T.A. Judge, E.A. Locke, C.C. Durham, and A.N. Kluger, "Dispositional effects on job and life satisfaction: the role of core evaluations," *J. Appl. Psychol.*, vol. 83, no. 1, p. 17, 1998, doi: 10.1037/0021-9010.83.1.17.

[17] Y. Zhang and P. Zhang, "Machine training and parameter settings with social emotional optimization algorithm for support vector machine," *Pattern Recognit. Lett.*, vol. 54, pp. 36–42, 2015, doi: 10.1016/j.patrec.2014.11.011.